Spatiotemporal pattern formation in neural systems with heterogeneous connection topologies

V. K. Jirsa* and J. A. S. Kelso
Center for Complex Systems and Brain Sciences, Florida Atlantic University, Boca Raton, Florida 33431
(Received 25 June 2000)

Biological systems like the human cortex show homogeneous connectivity, with additional strongly heterogeneous projections from one area to another. Here we report how such a dynamic system performs a macroscopically coherent pattern formation. The connection topology is used systematically as a control parameter to guide the neural system through a series of phase transitions. We discuss the example of a two-point connection, and its destabilization mechanism.

PACS number(s): 87.18.Sn, 47.54.+r, 82.40.Ck, 84.35.+i

A sheet composed of neurons or neural ensembles provides a medium for spatiotemporal pattern formation of neural activity. In contrast to typical pattern formation in physical or chemical systems [1,2], a neural system has a spatially variant connection topology in which a cortical area is not only connected to its nearest neighbors, but also has projections to distant areas. By these means the nervous system accomplishes a directed transfer of activity within a continuous sheet in which it would spread out uniformly otherwise. Such projections may not only serve to organize local dynamics within cortical areas such as synchronization of local rhythms, but also contribute to the macroscopic organization of neural activity or global dynamics. Neurobiological theories of memory are severely weakened by their inability to specify how changes in synaptic strength, the presumed agency in encoding, alter complex network operations, the presumed substrates of memory expression [3]. We address this problem for the dynamics on the network level such that any local dynamics is represented by a scalar activity resulting in a neural ensemble theory [5–8]. Local changes in synaptic weights, however, will alter the connectivity of the neural system, and by these means its global network dynamics. Here we wish to study the properties and mechanisms involved in the spatiotemporal neural pattern formation when the network's connection topology is varied. As an example we discuss a two-point connection embedded in a spatially continuous, homogeneously connected medium, and explain its underlying destabilization mechanism.

Following Jirsa and Haken [6], we define the spatiotemporal dynamics of a scalar neural field $\psi(x,t)$ with space $x \in \mathcal{R}^n$ and time $t \in \mathcal{R}$ as a nonlinear retarded integral equation of the form

$$\psi(x,t) = \int_A dX f(x,X) S[\psi(X,T) + I(X,T)], \qquad (1)$$

where $f(x,X)$ describes a general connectivity function, and S a nonlinear function of ψ at a space point X and a time point $T = t - |x-X|/v$, delayed by the propagation time over the distance $|x-X|$. A denotes the surface area of the medium, and v the constant signal velocity. $I(x,t)$ is the input to the field $\psi(x,t)$. Variations of this type of integral equation were widely used in theoretical neuroscience [4–8] to describe the dynamics of neural activity. However, in all these cases, as well as generally in physical and chemical systems, translational variance $f(x,X) = f_h(|x-X|)$ was employed. Here $f(x,X)$ will be typically decomposed into homogeneous contributions $f_h(|x-X|)$ and heterogeneous projections $f_i(x,X)$. We decompose the field $\psi(x,t)$ into spatial modes $g_n(x)$ and complex time dependent amplitudes $\psi_n(t)$ such as $\psi(x,t) = \Sigma_{n=-\infty}^{\infty} g_n(x)\psi_n(t)$. The choice of the spatial basis functions will depend on the surface A and its boundary conditions, but also on practical considerations about the type of connectivity $f(x,X)$ and inputs I to the system. We choose a polynomial representation of the nonlinear function S in Eq. (1) such as $S(X,T) = a_0 + a_1\psi(X,T) + a_2\psi^2(X,T) + \cdots = \Sigma_{m=0}^{\infty} a_m \psi^m(X,T)$, where $a_m \in \mathcal{R}$, and $I(X,T)$ is not considered (no restriction of generality). By projection of Eq. (1) onto a spatial basis function $\overline{g_q}(x)$, and restricting its dimension N to be finite, we obtain a set of N coupled integral equations

$$\begin{aligned}\Psi(t) &= v \int_{-\infty}^{t} d\tau [\Gamma_0(t-\tau) + \Gamma_1(t-\tau)\Psi(\tau) \\ &\quad + \Gamma_2(t-\tau)\Psi(\tau)\Psi(\tau) + \cdots] \\ &= v \int_{-\infty}^{t} d\tau \Gamma_0(t-\tau) + L^t\Psi(t) + N^t[\Psi(t)], \qquad (2)\end{aligned}$$

where vector notation has been used: $\Psi(t) = [\cdots \psi_q(t) \cdots]^T$, $\Gamma_0(t-\tau) = [\cdots \Gamma_q(t-\tau)\cdots]^T$, $\Gamma_1(t-\tau) = [\Gamma_{qn}(t-\tau)]$, $\ldots$. Formally L^t and N^t represent the linear and nonlinear temporal evolution operators, and $\Gamma_q(t-\tau)$ are tensor matrices composed of the spatial modes $g_q(x)$ and the connectivity function $f(x,X)$. A linear stability analysis of Eq. (2) yields the eigenvalue problem

$$\det[e^{-\lambda t} L^t(e^{-\lambda\tau}) - I] = 0, \qquad (3)$$

where I is the identity matrix. The entire complexity of the connection topology is contained in the tensor matrix $\Gamma_1(t-\tau)$, with $L^t = v\int_{-\infty}^{t} d\tau \Gamma_1(t-\tau)$, and the spatial basis functions. The elements of the tensor matrix $\Gamma_1(t-\tau)$ are $\Gamma_{qn}(t-\tau) = a_1(\gamma^- + \gamma^+)$, where

*Email address: jirsa@walt.ccs.fau.edu

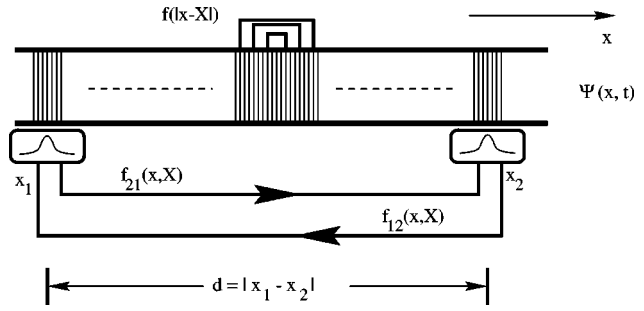

FIG. 1. The homogeneous connection topology is illustrated within a one-dimensional continuous medium whose activity is described by $\psi(x,t)$. A projection from x_1 to x_2 introduces a heterogeneity into the connectivity.

$$\gamma^{\pm}=\int_A dx\,\bar{g}_q(x)f[x,x\pm v(t-\tau)]g_n[x\pm v(t-\tau)]. \quad (4)$$

In a spatially invariant medium, the connectivity and the contribution of the spatial modes factorize, resulting in a separation of spatial and temporal constraints. However, this is not given when projecting pathways $f_i(x,X)$ are introduced into the neural sheet. Then truly spatiotemporal constraints for the linear stability exist such that $C_{qn}(x_0)=|\int_A dx\,\bar{g}_q(x)g_n(x\pm x_0)f_i(x,x\pm x_0)|$ represents a measure with $x_0=v(t-\tau)$ for the similarity between the spatial modes and the heterogeneous pathways. The necessary condition for destabilization of a pattern in Eq. (3) is $C_{qn}(x_0)>0$, such that only spatial modes may be destabilized that are sufficiently similar to the connectivity structure. The sufficient condition for destabilization is $\mathrm{Re}(\lambda)>0$ in Eq. (3).

The most elementary heterogeneous connection is a fiber connecting area x_1 to area x_2, because it is not only the simplest heterogeneity, but also the heterogenous connectivity matrix $f_i(x,x\pm x_0)$ may be reconstructed by the sum of such two-point connections between areas x_i and x_j such as $f_i(x,x\pm x_0)=\Sigma_{i,j}f_{ij}\delta(x-x_i)\,\delta(x-x_j\pm x_0)$, with the synaptic weight f_{ij} as a parameter. Typically such projections are bilateral [9], but not necessarily symmetric: $f_{ij}\neq f_{ji}$. Then the similarity measure $C_{qn}(x_0)$ can be written as

$$C_{qn}(x_0)=\left|\sum_{i,j} f_{ij}\bar{g}_q(x_i)g_n(x_i\pm x_0)\,\delta(x_i-x_j\pm x_0)\right|. \quad (5)$$

Realistically, the neocortex consists of many interareal two-point connections, leading to hierarchical signal processing shemes in a continuous neural sheet, of which the best known are the visual areas [9]. The brain provides a range of varying connectivity structures allowing flexibility for the same functions, generally assumed to be represented by network operations. Such variablility is found in the reorganization of neural function after brain injuries, which reflects major changes in connectivity [10]. However, the brain also provides mechanisms to alter these connectivities, such as long term potentiation [3], which vary the location of the terminals of pathways. An extraordinary, though pathological, example of stable and coherent global pattern formation in the brain network is found in epilepsies, which are often treated by changing its connectivity, i.e., by cutting the linking pathways of the hemispheres, the corpus callossum. In the following we wish to demonstrate how changes of the locations of a single pathway systematically control the pattern formation of the entire network. We embed a heterogeneous two-point connection between locations x_1 and x_2 in a one-dimensional homogeneous medium. Its connectivity function $f(x,X)$ shall be given by $f(x,X)=f(|x-X|)+f_{12}(x,X)+f_{21}(x,X)$, where f_{12} is the link from x_2 to x_1, and f_{21} the link in the opposite direction, as illustrated in Fig. 1. The distance between the inhomogeneous contributions of connectivity is $d=|x-X|$, which serves as our control parameter.

The dynamics of our example is given by Eq. (1), in which $\bar{\psi}(x,t)=\int_A dX\,\psi(X,t)$ is subtracted in the argument of the sigmoid S to reduce spatially uniform saturation effects [6,11]. Periodic boundaries are imposed. The connec-

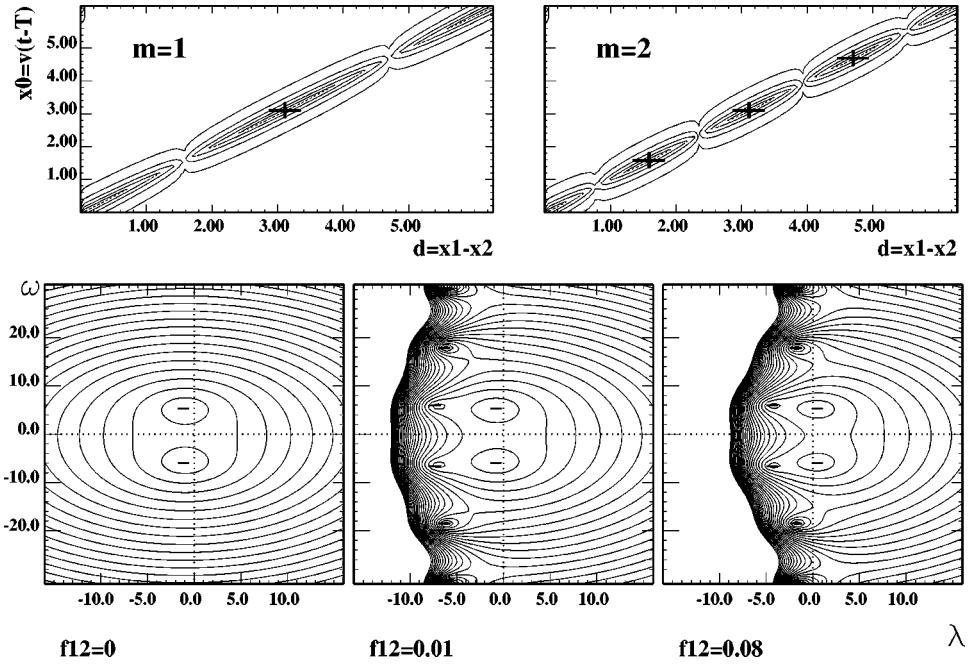

FIG. 2. In the top row, the similarity measure $C_{mm}(x_0)$ is plotted for the spatial patterns $m=1$ and 2, in dependence on x_0 and d. The plus signs show the maxima of similarity, and identify the regions in which a destabilization of an activity pattern may occur. In the bottom row, the eigenvalue of a pattern, as a solution of Eq. (6), is obtained graphically by the minima in the contour plots $\lambda-\omega$. As the synaptic strength $f_{12}=f_{21}$ is increased, the activity pattern is destabilized when its real part λ of the eigenvalue crosses the dotted zero line.

FIG. 3. The transition behavior of the system in Eq. (1) is plotted in a space-time diagram (horizontal time, vertical space). The originally stable spatiotemporal pattern is destabilized by moving the location of the heterogeneous projection from $x_2=B$ to $x_2=C$. The units used are the number of time steps and the arbitrary amplitude, respectively.

tivities are specified as $f(|x-X|)=(2\sigma)^{-1}\exp-|x-X|/\sigma$, $f_{12}(x,X)=1/2f_{12}\delta(x-x_1)\delta(X-x_2)$ and $f_{21}(x,X)=1/2f_{21}\delta(x-x_2)\delta(X-x_1)$, where σ, f_{12}, and f_{21} are constant parameters. We choose the spatial basis system to be spanned by the trigonometric functions $\sin nkx$ and $\cos mkx$, with $n,m\in\mathcal{Z}$ and $k=2\pi/L$, where L is the length of the one-dimensional closed loop. $x_1=0$ is not varied, thereby resulting in a pinning of the spatial modes around $x=0$. The nonlinear function S in Eq. (1) is assumed to be sigmoidal [6]. We study the stability of the origin $\Psi_0=0$, and expand S around its deflection point, $S[n]\approx\alpha n-4/3\alpha^3n^3\pm\cdots$. We consider a spatial basis function $g_m(x)=\cos mkx$ to second order in m, and truncate the expansion of the sigmoid after the third order to study small amplitude dynamics. The similarity measure $C_{mm}(x_0)$ is determined after Eq. (5), and plotted in dependence on x_0 and d for the first two spatial patterns $m=1$ and 2 in the top row of Fig. 2. The plus signs show the maxima of the spatiotemporal similarity, and identify the regions in which a destabilization of a pattern may occur. Following the eigenvalue problem in Eq. (3), we obtain a transcendental equation for the linear stability of the mth spatial mode,

$$\begin{aligned}&[(im\omega+\lambda_m)^2+2\omega_0(im\omega+\lambda_m)+\omega_0^2+m^2k^2v^2],\\&(1-d_1e^{(im\omega+\lambda_m)d/v})-(im\omega+\lambda_m+\omega_0)\omega_0\alpha=0,\end{aligned}\tag{6}$$

where $d_1=2\alpha/L(f_{12}+f_{21})\cos mkx_1\cos mkx_2$. The real part λ_m of its eigenvalue and its frequency ω can be determined graphically from Eq. (6) as functions of the control parameter d, and are shown in the bottom row of Fig. 2 for increasing synaptic strength $f_{12}=f_{21}$.

The destabilization of a particular state m depends on d_1 and d. For $d_1,d=0$, a purely homogeneous system is obtained in which the origin is the only stable state for sufficiently small α. The introduction of a heterogeneous projection $f_{ij}(x,X)$ may cause a desynchronization of the connected areas, and thus a destabilization of the respective spatial mode, resulting in a phase transition. As seen in Fig. 2 (bottom row), the complex conjugate pair of eigenvalues cross the dotted zero line, and their real parts become positive, for increasing synaptic strength $f_{12}=f_{21}$, causing a Hopf bifurcation.

To investigate this dynamics numerically, we prepare the system in a well-defined state, and change the connection topology by decreasing the control parameter $d=|x_1-x_2|$.

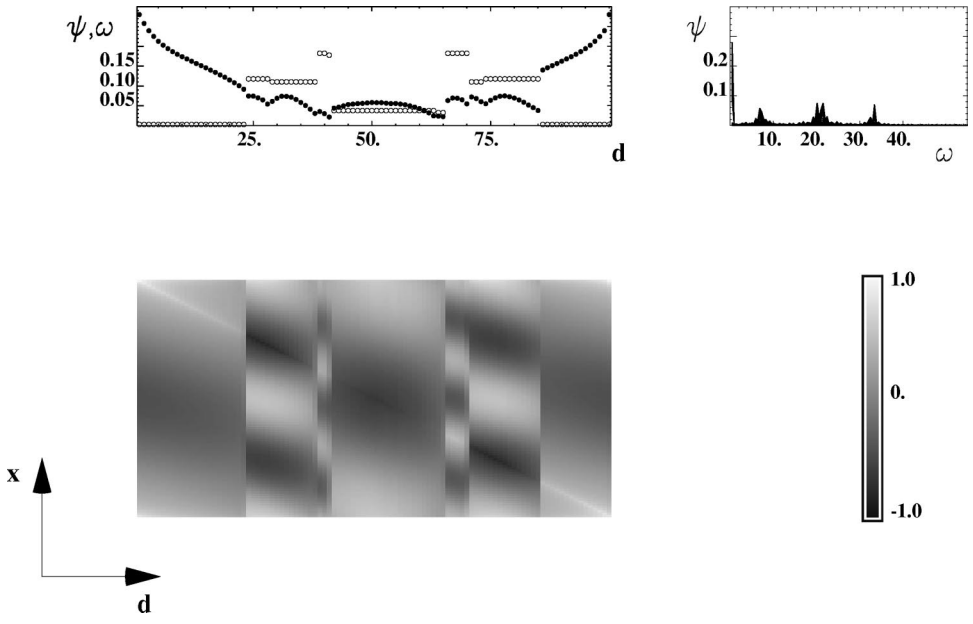

FIG. 4. The dominant spatial patterns for varying d are displayed in a spatiotemporal bifurcation diagram. The same amount of change in d, i.e., in the connectivity, can have entirely different effects depending on where these changes occur. For instance, an increase of d from 15 to 20 units does not show any qualitative changes in the dynamics, but an increase of d from 22 to 27 units causes a phase transition. Directly above, the amplitude (full circles) and temporal frequency (donuts) of the dominating pattern are plotted over the distance d. In the top right corner, the power spectra of the dominating patterns are plotted for all values of d.

Initially the system is prepared in a coherent oscillatory stationary state. Then the connectivity is changed by moving the terminal of the inhomogeneity at $x_2 = B$ to a new location $x_2 = C$, whereas the other terminal stays constant at $x_1 = A$. The change in the connection topology destabilizes the initial stationary dynamics, and the system undergoes a transition to a new stationary state. Without the inhomogeneous connections the zero-activity state is stationary and stable. The parameters used for the integration of Eq. (1) are $v = 3$, $\Gamma = \pi$, $a = 2.5$, $\sigma = 0.7$, $\sigma_1 = \sigma_2 = 0.1$, and $f_{12} = f_{21} = 1$. The time step is $dt = 0.02$, the space is divided into 100 units (see Fig. 3).

We investigate the dynamics in more detail by varying the control parameter d systematically from 0 to its maximal value $d = \Gamma$. Due to the periodic boundary conditions, a value $d > \Gamma/2$ reduces the relative distance between the inhomogeneities. The inhomogeneity at x_1 is kept constant, and $x_2 = x_1 + d$ is varied. For each distance d the system dynamics becomes stationary, and then the spatial pattern at maximum amplitude is extracted and plotted over d in a bifurcation plot. These patterns are normalized with respect to the largest amplitude. Under variation of d the system undergoes a series of spatiotemporal bifurcations. Note that these patterns are not harmonic due to the inhomogeneous connection topology. Shifts in the frequency spectra (plotted on the right for all distances d) are observed, even though the spatial pattern remains qualitatively the same. Hysteresis effects are found, resulting in an asymmetry of the bifurcation path below and above $d = \Gamma/2$. Above the bifurcation plot the corresponding amplitude (full circles) of the location x_1 and its temporal frequency are plotted (donuts) over d (see Fig. 4).

We described macroscopic coherent pattern formation in a spatially continuous neural system system with a heterogeneous connection topology. Local changes of connecting pathways may guide the neural system through a series of global spatiotemporal bifurcations.

This research was supported by NIMH and The Human Frontiers Science Project. V.K.J. wishes to thank Hermann Haken for interesting and helpful discussions.

[1] H. Haken, *Synergetics. An Introduction*, 3rd ed. (Springer, Berlin, 1983).
[2] M.C. Cross, P.C. Hohenberg, Rev. Mod. Phys. **65**, 851 (1993).
[3] *Synaptic Plasticity*, edited by M. Baudry, R.F. Thompson, and J.L. Davis (MIT Press, Cambridge, MA, 1993).
[4] S. Amari, Biol. Cybern. **27**, 77 (1977).
[5] P.L. Nunez, *Neocortical Dynamics and Human EEG Rhythms* (Oxford University Press, Oxford, 1995).
[6] V.K. Jirsa and H. Haken, Phys. Rev. Lett. **77**, 960 (1996).
[7] J.J. Wright and D.T.J. Liley, Behav. Brain Sci. **19**, 285 (1996).
[8] P.A. Robinson, C.J. Rennie, and J.J. Wright, Phys. Rev. E **56**, 826 (1997).
[9] D.J. Felleman and D.C. Van Essen, Cereb. Cortex **1**, 1 (1991).
[10] J. Fox, Science **225**, 820 (1984).
[11] V.K. Jirsa, A. Fuchs, and J.A.S. Kelso, Neural Comput. **10**, 2019 (1998).